of the 1-NAc group allows them to occupy the **A-1** and **N** loci (Figure 3b). In this case, the 3-OH group at **A-1** is galactosylated, as is actually observed. On the contrary, 1-NAc derivatives of D-sugars can not adopt the supplementary interaction at the **N** or **A-2** loci. Instead, D-xylose-1-NAc may adopt an alternative bonding at the **A-2** and **N** loci where no reactive OH is placed at **A-1** (Figure 3c). For D-glucose-1-NAc, which is reactive in the presence of α-LA, the exocyclic C-5 group may disturb this bonding (Figure 3d). Moreover, judging from the higher reactivity of D-glucose than D-xylose (Figure 1a), a peripheral binding interaction may exist around the C-5 group of D-glucose and contribute to the usual β-1,4-transfer reaction.

In conclusion, we have proved that an anomeric NAc group changes unnatural L-glucose and L-xylose into acceptor substrates for bovine β-1,4-GalTase. The transfer reaction is regiospecific at the 3-OH position and so this is the first β-1,3-transfer reaction for this enzyme. This finding, together with our previous ones, have shown that variable unnatural glycosyl linkages can be produced enzymatically by a single enzyme. This fact may exceed the general concepts of "one glycosyl enzyme for one glycosyl linkage"[13] and "biological homochirality"[14] that express the high substrate and enantiospecificity of enzyme reactions in biosynthetic pathways.

Received: September 24, 1999 [Z14064]
Revised: January 31, 2000

[1] a) C.-H. Wong, R. L. Halcomb, Y. Ichikawa, T. Kajimoto, *Angew. Chem.* **1995**, *107*, 559; *Angew. Chem. Int. Ed. Engl.* **1995**, *34*, 521 – 546; b) M. M. Palcic, O. Hindsgaul, *Trends Glycosci. Glycotechnol.* **1996**, *8*, 37 – 49.
[2] K.-Y. Do, S.-I. Do, R. D. Cummings, *J. Biol. Chem.* **1995**, *270*, 18447 – 18451.
[3] Y. Nishida, T. Wiemann, V. Sinnwell, J. Thiem, *J. Am. Chem. Soc.* **1993**, *115*, 2536 – 2537.
[4] a) Y. Nishida, T. Wiemann, J. Thiem, *Tetrahedron Lett.* **1992**, *33*, 8043 – 8046; b) Y. Nishida, T. Wiemann, J. Thiem, *Tetrahedron Lett.* **1993**, *34*, 2905 – 2906.
[5] T. Wiemann, Y. Nishida, V. Sinnwell, J. Thiem, *J. Org. Chem.* **1994**, *59*, 6744 – 6747.
[6] L. M. Likhosherstov, O. S. Novikova, V. A. Derevitskaja, N. K. Kochetkov, *Carbohydr. Res.* **1986**, *146*, C1 – C5.
[7] D. K. Fitzgerald, B. Colvin, R. Marval, K. E. Ebner, *Anal. Biochem.* **1970**, *36*, 43 – 61.
[8] a) R. U.Lemieux, *Chem. Soc. Rev.* **1989**, *18*, 347 – 374; b) M.-H. Du, U. Spohr, R. U. Lemieux, *Glycoconjugate J.* **1994**, *11*, 443 – 461.
[9] Y. Kajihara, H. Kodama, T. Endo, H. Hashimoto, *Carbohydr. Res.* **1998**, *306*, 361 – 378.
[10] a) K. Drickamer, *Nature* **1992**, *360*, 183 – 186; b) K. Drickamer, *J. Biol. Chem*. **1988**, *263*, 9557 – 9560.
[11] L. J. Berliner, M. E. Davies, K. E. Ebner, T. A. Bayer, J. E. Bell, *Mol. Cell. Biochem.* **1984**, *62*, 37 – 42.
[12] J. A. Grobler, M. Wang, A. C. W. Pike, K. Brew, *J. Biol. Chem.* **1994**, *269*, 5106 – 5114.
[13] S. Natsuka, J. B. Lowe, *Curr. Opin. Struct. Biol.* **1994**, *4*, 683 – 691.
[14] a) V. V. Avetisov, V. I. Goldanskii, *BioSystems* **1991**, *25*, 141 – 150; b) J. M. Bailey, *FASEB J.* **1998**, *12*, 503 – 507.
[15] H. Ohrui, Y. Nishida, H. Itoh, H. Hori, H. Meguro, *J. Org. Chem.* **1991**, *56*, 1726 – 1731.

Two-State Reactivity in the Rebound Step of Alkane Hydroxylation by Cytochrome P-450: Origins of Free Radicals with Finite Lifetimes**

Nathan Harris, Shimrit Cohen, Michael Filatov, François Ogliaro, and Sason Shaik*

Alkane hydroxylation[1] by cytochrome P-450 poses tantalizing mechanistic questions. The consensus rebound mechanism, Scheme 1,[2] involves hydrogen abstraction from the

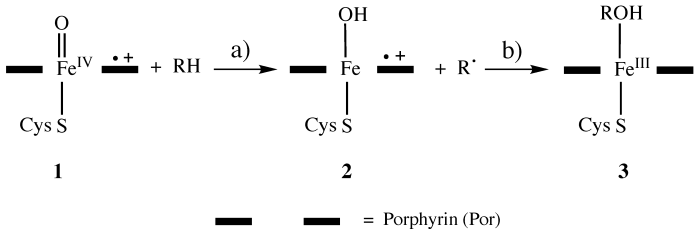

Scheme 1. Schematic representation of the rebound mechanism.

alkane (RH) in step (a), followed by hydroxyl rebound onto the radical to generate the ferric – alcohol complex, in step (b). The rebound mechanism has gained support from findings of rearranged alcohol products, which indicate the presence of a free radical with a finite lifetime.[3] Further support has recently been provided by the kinetic isotope effect (KIE) measurements of Dinnocenzo, Jones et al.[4a] They found that for a few substituted alkanes, the KIE's of cytochrome P-450 hydroxylation are virtually identical to those of a corresponding hydrogen abstraction reaction by *tert*-butoxyl radical, thus implying isostructural transition states for the two processes.[4] In an apparent contrast, mechanistic studies by Newcomb and co-workers,[5] designed to probe the radical using alkane substrates that would yield ultrafast radical clocks, do not concur with a free-radical intermediacy; apparent lifetimes are too fast to correspond to a real free-radical intermediate (for example, $\tau \leq 70$ fs),[5b] and have no correlation with independently clocked rearrangement lifetimes of the free radicals.[5a] Thus, while the evidence for incursion of radicals is strong, their presence is nevertheless controversial and merits elucidation.

The origin of the radicals in the rebound process is the key issue addressed in this communication. Our approach to tackle this question, is to use density functional calculations to ascertain whether the hypothetical rebound process in step (b) of Scheme 1, involves a barrier which would endow the

[*] Prof. S. Shaik, Dr. N. Harris, S. Cohen, Dr. M. Filatov, Dr. F. Ogliaro
Department of Organic Chemistry and
The Lise Meitner-Minerva Center for Computational Quantum Chemistry
Hebrew University, 91904 Jerusalem (Israel)
Fax: (+972) 2-658-5345
E-mail: sason@yfaat.ch.huji.ac.il

[**] This research was sponsored by the Israeli Science Foundation (ISF) and, in part, by the German Israeli Foundation (GIF), and the VW Stiftung. S.S. thanks the Humboldt Foundation for a Senior Research Award. F.O. thanks the EU for a Marie Curie Fellowship.

radical with a finite lifetime, and if so what is the precise nature of the iron–porphyrin state that originates the barrier? Thus, our study focuses on modeling of the rebound process itself, and is not meant to be a study of the full hydroxylation mechanism of a particular alkane.

In a previous paper,[6] we showed by means of density functional calculations, that in a dielectric environment (such as in a solvent or in a protein cavity) the iron–hydroxo intermediate **2** in Scheme 1 involves an Fe^{III} (d^5 configuration) ion and a cation radical situated in the porphyrin. The ground state of the iron–hydroxo complex was found to be the triplet state ($S=1$) with single electrons occupying the $d_{yz}(\pi^*)$ orbital of the iron and the a_{2u} type orbital of the porphyrin, which is delocalized toward the sulfur.[6b] As shown in part (a) of Scheme 2, this iron–hydroxo complex with two unpaired

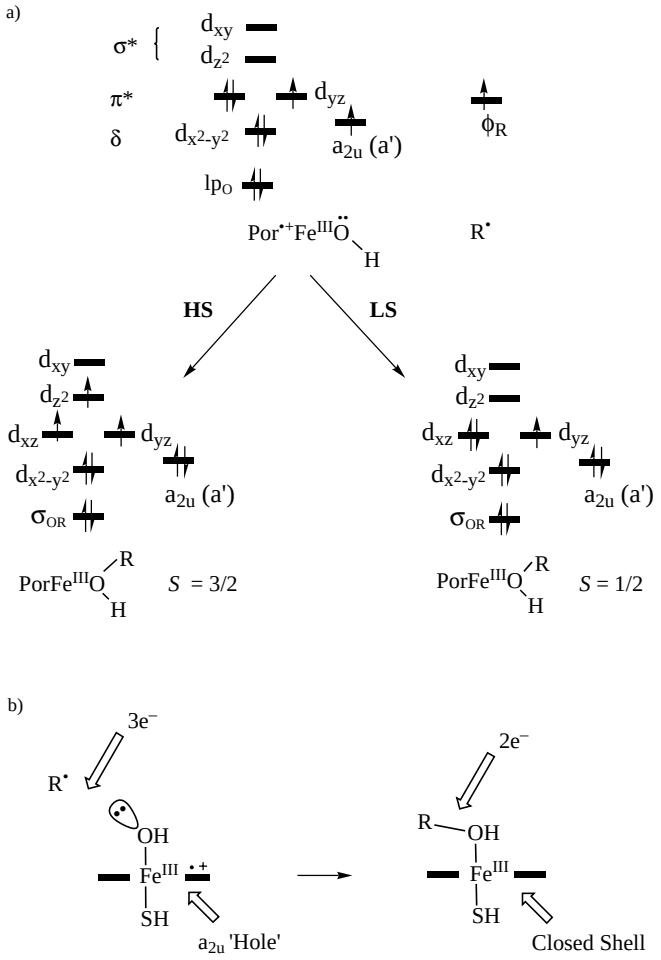

Scheme 2. a) Orbital diagrams showing the low-spin and high-spin coupling modes of the triplet iron–hydroxo and alkyl radical species during the rebound step. b) An electron-counting diagram illustrating the filling of the porphyrin "hole".

electrons in a triplet situation ($S=1$) can couple with the odd electron of the radical ($S=\frac{1}{2}$) in low-spin (LS) and high-spin (HS) manners, resulting in doublet ($S=\frac{1}{2}$) and quartet ($S=\frac{3}{2}$) states of the ferric–alcohol products, respectively. These two processes are studied here and, as will be shown, the radical has a finite lifetime due to a barrier on the high-spin surface, while the low-spin coupling proceeds to the ferric–alcohol complex with no significant barrier. This and the spin-state branching ratio[7] may well be the roots of the apparent controversy in the experimental data.

Hybrid (Hartree–Fock/DFT) density functional B3LYP calculations[8] are performed with the JAGUAR 3.5[9] and GAUSSIAN98[10] packages, and used for geometry optimization of the species in Scheme 1 with $CH_3^{\bullet}$ as a model radical and HS^- as an axial ligand. Following the previous study[6], we use the Los Alamos effective core potential coupled with the double zeta LACVP basis set[11] for iron, and an all-electron 6-31G basis set for the rest of the atoms. Molecular geometries of all species are fully optimized without any symmetry constraints.

For the ferric–methanol complex **3** (R = Me in Scheme 1), the ground state is found to be the doublet state ($S=\frac{1}{2}$) with the quartet state ($S=\frac{3}{2}$) lying 7.5 kcal mol^{-1} higher.[12] While transient alcohol complexes have not as yet been detected in a mechanistic study of the hydroxylation process, ferric–alcohol complexes of cytochrome P-450 are nevertheless known. Our computational result is in accord with the experimental assignment of the 5-hydroxycamphor complex (a ferric–alcohol complex) of cytochrome $P\text{-}450_{cam}$ as a doublet-spin complex ($S=\frac{1}{2}$).[13] The strong binding, indicated by the short Fe–O bond in the computed ferric–methanol complex (see Figure 1), suggests that an alcohol transient is reasonable,

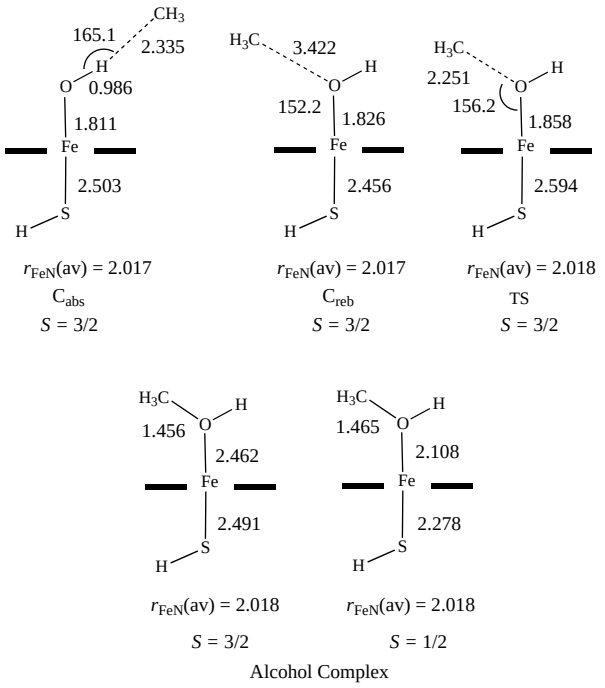

Figure 1. Stationary species for the rebound process.

while the alternative direct OH transfer to the alkyl radical to form a free alcohol may be energetically more demanding.[14]

From this point on, the term low spin (LS) will denote the doublet state while the term high spin (HS) will denote the quartet state.[12a] The HS rebound step involves a cluster that precedes a transition state (TS) en route to the HS ferric–methanol complex. These stationary species are depicted

  0570-0833/00/3911-2004 $ 17.50+.50/0 *Angew. Chem. Int. Ed.* **2000**, *39*, No. 11

schematically in Figure 1 which shows only key geometric parameters. The cluster C_{abs} is seen to correspond to the product of the hydrogen-abstraction step. Rotation of the methyl group to the other side of the oxygen occurs at the expense of a small energy increase (2.1 kcal mol^{-1}) and generates a second cluster, C_{reb}, which is not a true minimum but is a species en route to the rebound. In contrast, the only stationary point found in the LS rebound is the LS ferric–methanol product.

Location of the transition states on the HS and LS surfaces was achieved in two steps. First, the minimum energy HS and LS paths were scanned along the $r_{C\cdots O}$ coordinate (approach of the CH_3 radical to the oxygen of the iron–hydroxo complex) with C_s symmetry constraints. Figure 2 shows the energy

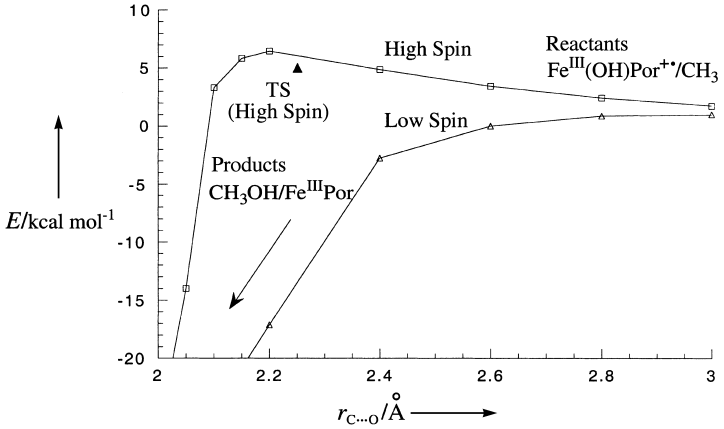

Figure 2. Potential energy curves of the high-spin (HS) and low-spin (LS) rebound processes along the $CH_3\cdots O$ coordinate ($r_{C\cdots O}$).

profiles obtained and it is apparent that, while the LS profile descends smoothly[15] toward the LS ferric–methanol complex, the HS surface exhibits a barrier near $r_{C\cdots O} = 2.2$ Å. The true transition state (TS) on the HS surface (shown with a filled triangle in Figure 2) was then located by saddle-point optimization of all geometric variables with no symmetry constraints. This was followed by a complete vibrational analysis which revealed that there is only one mode with an imaginary frequency of i447.6 cm^{-1} which corresponds to the expected mode along the $r_{C\cdots O}$ reaction coordinate that connects reactants to products.

Table 1 displays key features of the stationary structures along the path. The barrier relative to the separated fragments is 5.0 kcal mol^{-1}, and relative to the reactant cluster it is 7.1 kcal mol^{-1}. Considering the known tendency of density functionals to underestimate barriers,[16] the HS barrier feature found in this way is not likely to be an artifact. The energy stabilization of the LS surface in the region of the HS transition state (approximately 17 kcal mol^{-1} relative to the onset at 3 Å) is significantly larger than the expected B3LYP error.[16d] Thus, even if B3LYP overestimates the LS state somewhat, a significant barrier is still unlikely on the LS surface. We cannot however, rule out a tiny barrier at a much "earlier" position along the $r_{C\cdots O}$ coordinate.

Further inspection of Table 1 reveals that the HS TS possesses geometric parameters between those of the ferryl–hydroxo reactant complex, [Por$^{\bullet+}$Fe^{III}OH], and those of the HS ferric–methanol complex, [PorFe^{III}(CH$_3$OH)]. The spin density data in Table 1 further show that the vicinity of the TS is characterized by an extensive electronic reorganization. We shall now analyze this electronic reorganization, and thereby show that there is a simple reason for the HS barrier and the lack of an LS barrier.

Table 1 shows that the attacking $CH_3^{\bullet}$ radical and the porphyrin ring lose their initial spins in both the HS and LS rebounds. What makes the difference is the spin density of the iron, which rises steeply on the HS path (0.85–2.42), but remains essentially constant (0.84–0.86) along the LS path. The orbital diagrams, part (a) of Scheme 2, show the origins of this reorganization. Thus, initially in the ferryl–hydroxo reactant complex the $a_{2u}(a')$ porphyrin orbital[6b] is singly occupied, and so is the orbital of the alkyl group (lp_O is an oxygen lone-pair orbital). During the rebound, the $a_{2u}(a')$ orbital is filled by an electron formally provided by the alkyl radical R$^{\bullet}$ which now participates in the newly formed σ_{OR} orbital. However, while in the LS process this is the primary change, during the HS process the filling of the porphyrin shell must be attended by excitation of an electron from the d_{xz} orbital to the higher energy (σ^* type) d_{z^2} orbital. Thus, whereas in the iron–hydroxo complex/$CH_3^{\bullet}$ cluster all the unpaired electrons reside in relatively low-lying orbitals, in

Table 1. Selected geometric parameters r [Å], spin densities ρ, and relative energies E_{rel} [kcal mol^{-1}] of the critical species along the rebound pathway.

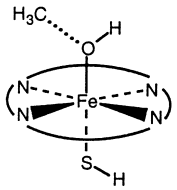

parameter	[Por$^{\bullet+}$Fe^{III}OH]/CH$_3^{\bullet}$ reactants	[Por$^{\bullet+}$Fe^{III}OH]/CH$_3^{\bullet}$ HS cluster[a]	TS HS	[PorFe^{III}(CH$_3$OH)] HS	[PorFe^{III}(CH$_3$OH)] LS
$r_{C\cdots O}$	∞	3.298	2.251	1.456	1.465[b]
r_{Fe-O}	1.824 (1.829)[d]	1.811	1.858	2.462	2.108[c]
r_{Fe-S}	2.490 (2.458)[d]	2.503	2.594	2.491	2.278
r_{Fe-N}(av)[e]	2.017 (2.017)[d]	2.017	2.018	2.018	2.018
$r_{Fe\text{-}ring}$	+0.09	+0.09	+0.08	−0.14	−0.09
E_{rel}	0	−2.1	+5.0[f] −17.1[g]	−61.2	−68.7
ρ_{CH_3}	0.99	0.96	0.66–0.33 [h]	0.003	0.000
ρ_{ring}	0.67	0.52	0.66–0.13[h]	0.18	0.032
ρ_{Fe}	0.85	0.84	1.05–2.26[h]	2.42	0.86

[a] The C_{abs} cluster shown in Figure 1. [b] C–O distance. [c] Fe$\cdots$O distance. [d] Data in parentheses are for the C_s structure[6] which is 0.88 kcal mol^{-1} higher than the C_1 structure (data not in parentheses). [e] The average measurements of four Fe–N distances. [f] The barrier relative to the optimized reactant at C_1 symmetry. [g] Energy of the corresponding LS structure at 2.2 Å. [h] Range of spin density at $r_{C\cdots O} = 2.2$–2.05 Å.

  0570-0833/00/3911-2005 $ 17.50+.50/0

the HS TS and in the corresponding HS ferric–alcohol complex, one electron is excited to a higher level $\sigma^*(d_{z^2})$ orbital in order to conserve the total quartet spin. This additional excitation is accompanied by the aforementioned increase of the spin density on the iron, as well as by a considerable elongation of the Fe–O and Fe–S bond lengths in the TS relative to the iron–hydroxo complex, and the loss of bonding is manifested as a barrier for the HS rebound process. Thus, the barrier on the HS path has a straightforward electronic origin.

Since the LS path is barrier-free, or very flat, it cannot endow a radical intermediate with a significant lifetime, if at all. It follows that LS hydroxylation will proceed in an effectively concerted manner,[5b, 7, 17] even if the trajectory of approach of the ferryl–oxene species to the R–H alkane will resemble a hydrogen abstraction process. Along the same trajectory, an alkyl radical will be produced on the HS path and will face a rebound barrier. Thus, assuming that the rate of the rebound step obeys the Arrhenius equation with the same preexponential factor for the HS and LS pathways, the potential barrier of 5 to 7 kcal mol^{-1} on the HS profile will slow down the HS rebound by four to six orders of magnitude, and will thereby endow the radical with a significant lifetime, during which radical rearrangement can occur. In this dual pathway scenario, where rearranged alcohol is produced through only one state (HS), while unrearranged alcohol is produced from two states (LS and HS), apparent lifetimes—calculated from percentages of rearrangement—may occasionally appear unrealistically short and will bear no correlation to clocked lifetimes of the free radicals, as observed by Newcomb et al.[5] At the same time, the measured KIE will reflect a "hydrogen abstraction trajectory" (common to the two states), as deduced in the study by Dinnocenzo, Jones et al.[4] Thus, the proposed two-state scenario provides a reasonable reconciliation of the apparent contradiction in the two sets of data.

The percentage of rearrangement will depend on the initial concentration of the radical, as determined by the branching ratio of the reaction complexes between the HS and LS processes,[7] as well as on the HS rebound rate, which is sized by the HS barrier. Two factors will influence the height of the barrier in the HS rebound, and can be deduced from Scheme 2. The first factor is associated with the electron excitation from the lower level d_{xz} orbital to the higher energy $d_{z^2}(\sigma^*)$ orbital which is antibonding across the axial O-Fe-S axis. The stronger the S-binding ability of the thiolate ligand, the higher the $d_{z^2}(\sigma^*)$ orbital is, and a higher HS rebound barrier is the result. Since in the natural enzyme the thiolate ligand is a side group of the encapsulating protein, the protein is expected to affect the binding ability of the thiolate through variation in the polarity and acidity of its pocket as well as through steric constraints for Fe–S bonding.

The second factor of the rebound barrier is associated with the properties of the attacking radical and can be deduced from part (b) of Scheme 2. A simple electron count reveals that, initially, the R–O linkage involves three electrons and the porphyrin has a "hole",[6b] and later the R-O linkage becomes a two-electron R–O bond and the porphyrin attains a closed shell. Thus, the electron that fills the porphyrin "hole" originates in the extra electron of the R–O linkage and is formally transferred from the electropositive alkyl radical. Consequently, the HS rebound process involves concomitantly an R–O bond formation and an electron shift (from R$^{\bullet}$ to Por$^{\bullet+}$). It follows therefore that the percentage of radical rearrangement will depend on the oxidation potential of the radical. All other factors being equal, the lower the oxidation potential, the shorter the true lifetime of the radical on the HS surface and the less rearranged alcohol can be expected. This trend is in agreement with recent observations by Newcomb et al., who found that as the alkyl radical moiety of the substrates (2-aryl-cyclopropyl alkanes) becomes a better electron donor, the amount of rearranged alcohol decreases from 26% (for a *p*-CF_3 aryl substituent) down to less than 1% for the best donor situation (for 2-phenyl-cyclopropyl isopropane).[5c] Nevertheless, the experimental results are more complicated due to rearrangement of cationic intermediates and the presence of more than one oxidizing species.[5]

Received: September 1, 1999 [Z13948]
Revised: November 22, 1999

[1] M. Sono, M. P. Roach, E. D. Coulter, J. H. Dawson, *Chem. Rev.* **1996**, *96*, 2841.
[2] a) J. T. Groves, *J. Chem. Educ.* **1985**, *62*, 928; b) J. T. Groves, G. A. McClusky, *J. Am. Chem. Soc.* **1976**, *98*, 859.
[3] a) J. T. Groves, Y.-Z. Hang in *Cytochrome P450: Structure, Mechanisms and Biochemistry*, 2nd ed. (Ed.: P. R. Ortiz de Montellano), Plenum, New York, **1995**, chap. 1; b) B. Meunier, *Chem. Rev.* **1992**, *92*, 1411; c) W. D. Woggon, *Top. Curr. Chem.* **1996**, *184*, 40.
[4] a) J. I. Manchester, J. P. Dinnocenzo, L. A. Higgins, J. P. Jones, *J. Am. Chem. Soc.* **1997**, *119*, 5069; b) The dimethyl aniline substrates in ref. [4a] were suggested later to undergo an initial electron transfer by the ferryl–oxene species of horseradish peroxidase and by a synthetic ferryl–oxene model (Y. Goto, Y. Watanabe, S. Fukuzumi, J. P. Jones, J. P. Dinnocenzo, *J. Am. Chem. Soc.* **1998**, *120*, 10762). This conclusion does not, however, pertain to the toluene, *p*-xylene, and benzyl alcohol species in ref. [4a]. Furthermore, all the model ferryl–oxene systems, used in the study, are better electron acceptors than the cytochrome P-450 ferryl–oxene complex so that the results may not pertain at all to oxidation by cytochrome P-450.
[5] a) M. Newcomb, M.-H. Le Tadic, D. A. Putt, P. F. Hollenberg, *J. Am. Chem. Soc.* **1995**, *117*, 3312; b) M. Newcomb, M.-H. Le Tadic-Beadatti, D. L. Chestney, E. S. Roberts, P. F. Hollenberg, *J. Am. Chem. Soc.* **1995**, *117*, 12085; c) P. H. Toy, M. Newcomb, P. F. Hollenberg, *J. Am. Chem. Soc.* **1998**, *120*, 7719.
[6] a) M. Filatov, N. Harris, S. Shaik, *Angew. Chem.* **1999**, *111*, 3730; *Angew. Chem. Int. Ed.* **1999**, *38*, 3512. The paper shows that in the gas phase the electromeric forms, [PorFe^{IV}OH] ($S=1$) and [Por$^{\bullet+}$Fe^{III}OH] ($S=1$) are almost degenerate, but a dielectric environment makes [Por$^{\bullet+}$Fe^{III}OH] ($S=1$) the ground state. This is in accord with electrochemical results in: J. T. Groves, Z. Gross, M. K. Stern, *Inorg. Chem.* **1994**, *33*, 5065. b) The spin density is 67% in the porphyrin and 30% on the thiolate ligand for the model thiolate used here. This model is closer to the full cysteinato ligand than, for example, the CH_3S^- model.
[7] S. Shaik, M. Filatov, D. Schroder, H. Schwarz, *Chem. Eur. J.* **1998**, *4*, 193.
[8] P. J. Stevens, F. J. Devlin, C. F. Chablowski, M. J. Frisch, *J. Phys. Chem.* **1994**, *98*, 11623.
[9] JAGUAR 3.5, Schrodinger, Inc., Portland, OR, **1998**. The program employs the restricted open-shell B3LYP method.
[10] GAUSSIAN98, Gaussian, Inc., Pittsburgh, PA, **1998**.
[11] J. P. Hay, W. R. Wadt, *J. Chem. Phys.* **1985**, *82*, 299.
[12] a) The state with maximum spin ($S=5/2$) did not converge in our calculations. However, it must be kept in mind that whether the ground state of the product ferric–alcohol complex is $S=5/2$ or $S=1/2$ does not have bearing on the conclusions of this study, as summarized

  0570-0833/00/3911-2006 $ 17.50+.50/0

in Figure 2. What matters is the behavior of states obtained by the two spin coupling modes in Scheme 2. b) Density functional calculations of corresponding ferric–water complexes give $S = ½$ ground state and a higher energy $S = 5/2$ state. See: M. Filatov, N. Harris, S. Shaik, *J. Chem. Soc. Perkin Trans. 2* **1999**, 399; M. T. Green, *J. Am. Chem. Soc.* **1998**, *120*, 10772. This is supported by experimental assignment. See: H. Thomann, M. Bernardo, D. Goldfrab, P. M. H. Kroneck, V. Ulrich, *J. Am. Chem. Soc.* **1995**, *117*, 8243. However, a recent experimental investigation of a model compound with a spatially fixed thiophenoxy ligand shows an $S = 5/2$ ground state and indicates the role of the protein in stabilizing the $S = ½$ ground state, as predicted initially by Harris and Loew. See: H. Aissaoui, R. Bachmann, A. Schweiger, W.-D. Woggon, *Angew. Chem.* **1998**, *110*, 3191; *Angew. Chem. Int. Ed.* **1998**, *37*, 2998; D. Harris, G. H. Loew, *J. Am. Chem. Soc*. **1993**, *115*, 8775.

[13] H. Li, S. Narashmhulu, L. M. Havran, J. D. Winkler, T. L. Poulos, *J. Am. Chem. Soc.* **1995**, *117*, 6297.

[14] A direct OH transfer mechanism would entail spin-state crossing to the $S = 5/2$ state of the five-coordinate ferric complex (for example, see: ref. [1]).

[15] All HS data are obtained with B3LYP using JAGUAR 3.5 (ref. [9]). The LS profile is calculated with the unrestricted B3LYP method in GAUSSIAN 98 (ref. [10]). For convenience, the zero of the energy scale in Figure 2 is common to the LS and HS curves.

[16] a) M. Filatov, W. Thiel, *Chem. Phys. Lett*. **1998**, *295*, 467; b) H. Basch, S. Hoz, *J. Phys. Chem. A* **1997**, *101*, 4416; c) S. Skokov, R. A. Wheeler, *Chem. Phys. Lett.* **1997**, *271*, 251; d) The average underestimation error of B3LYP (in ref. [16a–c]) for related reactions involving radicals is ≤ 6 kcal mol^{-1}, while for related reactions involving OH and CH_3 groups, the error is 0.5 kcal mol^{-1}.[16c] For reactions involving Fe, O, and H atoms, the underestimation error of the B3LYP barrier is approximately 1 kcal mol^{-1} relative to experimental data and 5.4 kcal mol^{-1} relative to the CASPT2 result which seems to overestimate the barrier.[17]

[17] M. Filatov, S. Shaik, *J. Phys. Chem. A* **1998**, *102*, 3835.

Redirecting Secondary Bonds To Control Molecular and Crystal Properties of an Iodosyl- and an Iodylbenzene**

Dainius Macikenas, Ewa Skrzypczak-Jankun, and John D. Protasiewicz*

Noncovalent, attractive interactions are extremely important forces that can influence molecular, solution, and solid-state properties. For example, hydrogen bonding is unarguably the most important directing intermolecular force and structure generating motif in many chemical and biological systems. Much less appreciated (and utilized) are the related forces that exist between heavier atoms. A class of such attractive interactions have often been termed secondary bonds.[1] Like hydrogen bonds, these bonds have strong electrostatic components and show directional preferences.[2] From the similarity to hydrogen bonds, it has also been suggested that secondary bonds might have potential for the rational design of supramolecular structures.[3]

Secondary bonds, particularly I···O bonds, are a pervasive feature of structural organoiodine(III) chemistry.[4] Recently, such secondary bond interactions have been exploited to introduce chiral environments about iodine(III) centers for enantioselective oxidation reactions.[5] In other cases, secondary bonds can be counterproductive. In iodosylbenzene $(PhIO)_n$, I···O bonds dominate the structure to such an extent that this extremely potent and important reagent is essentially insoluble in all nonreactive media.[6] Nonetheless, this veritable "oxygen atom warehouse" has found widespread use in catalytic oxygenation reactions after the discoveries of its efficacy as a source of oxygen atoms for oxidations catalyzed by cytochrome P-450[7] and by discrete transition metal complexes.[8]

Though known for over 100 years,[9] structural details for iodosylbenzene—or any members of this class of materials—are still limited. Various spectroscopic studies have suggested that iodosylbenzene adopts the form of a zigzag polymer (Scheme 1),[10] whereby monomeric units of PhIO are linked by intermolecular I···O secondary bonds. Within PhIO monomers, I–O single bonds (2.04 Å) and a C-I-O bond angle near 90° have been deduced from extended X-ray absorption fine-structure (EXAFS) analysis.[10g] The tight, solid-state aggregation of the PhIO monomers is undoubtedly caused by the strong electrostatic attractions between the oppositely charged iodine and oxygen atoms (right resonance structure, Scheme 1). Polymeric iodosylbenzene is also likely to be terminated by addition of water and thus iodosylbenzene can be further formulated as $HO(PhIO)_nH$.[11] We have recently discovered that soluble derivatives of (tosyliminoiodo)benzene and iodosylbenzene are realized if strong internal dipoles capable of introducing *intramolecular* I···O secondary bonds, for the purpose of replacing *intermolecular* I···N and I···O secondary bonds, are incorporated into these materials.[12] Indeed, a single-crystal X-ray structure analysis of the (tosyliminoiodo)benzene derivative showed the presence of significant intramolecular I···O secondary bonding and thus confirmed our expectations. We now have succeeded in obtaining single crystals suitable for X-ray diffraction studies of the corresponding soluble iodosylbenzene and herein report the first crystal structure of an iodosylbenzene derivative ArIO (**1**; $Ar = 2\text{-}t\text{BuSO}_2C_6H_4$). Furthermore, the crystal structure of the corresponding iodylbenzene $ArIO_2$ (**2**) has also been obtained. Comparisons between these two structures reveal interesting aspects of the nature of iodosyl and iodoxy bonds.

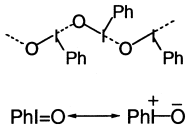

Scheme 1. Zigzag structure of iodosylbenzene.

[*] Prof. J. D. Protasiewicz, D. Macikenas
Department of Chemistry
Case Western Reserve University
10900 Euclid Avenue
Cleveland, OH 44106-7078 (USA)
Fax: (+1) 216-368-3006
E-mail: jdp5@po.cwru.edu
Dr. E. Skrzypczak-Jankun
Department of Chemistry
University of Toledo
Toledo, OH 43606-3390 (USA)

[**] This work was supported by the donors of The Petroleum Research Fund, administered by the American Chemical Society, and by the Ohio Board of Regents (for financial support of the Ohio Crystallographic Consortium).

  0570-0833/00/3911-2007 $ 17.50+.50/0